Removal of Malachite Green using Green Synthesized α-MnO2 nanoparticles: Kinetics, Intraparticle Diffusion and Isotherm

Annu T Mathew, Saravanakumar MP

Abstract*: This study helps to understand the adsorption of Malachite Green (MG) on α-MnO2 nanoparticles which was green synthesized using sugarcane juice. Different parameters including pH of solution, dosage of adsorbent, concentration of pollutant and time for adsorption process was studied to conclude the efficacy of the process using the adsorbent. The isotherm and kinetics for adsorption of MG concluded that Langmiur isotherm and pseudo second order kinetic model yields the best fit. The maximum monolayer sorption according to Langmiur was found to be 300.03 mg/g. So, α-MnO2 nanoparticles prove to be a cost effective, environment friendly and easily available 3D adsorbent.

Keywords*: Malachite Green, α-MnO2 nanorods, green synthesis, Kinetic study.

I. INTRODUCTION

Dyes disposed from textile industries into the water bodies without treatment affects the environment adversely and at the same time is not aesthetically acceptable. Malachite Green (MG) is an organic dye which exhibits resistance towards fading when exposed to light due to its complex structure preventing chemical precipitation or biological treatment for its removal[1]. This dye has been used not only in textile industry but also it finds application as a food coloring agent and a food additive. The utilization of MG has been banned in various parts of the world but it is still being used in many countries due to its efficiency and cost effectiveness[2]. People tend to suffer from carcinogenesis, teratogenesis, mutagenesis, reduced fertility and respiratory toxicity when exposed to MG polluted water [3]. Most of the water pollutants present in wastewater gets in the food chain leading to bioaccumulation and posing a serious threat to the environment[4].

An increase in use of agricultural and other naturally occurring products as adsorbents in the process of adsorption have been a part of recent researches due to its inexpensive, easy availability and eco-friendly nature. The green synthesis of nanoparticle has overcome the limitation of conventional physical and chemical methods and have proved to be a better alternative[5], [6]. Green synthesis basically aims at the application of sustainable processes for the elimination of hazardous wastes and utilization of environment friendly renewable solvents and chemicals. This work emphasizes on (i) Removal of MG using green synthesized αMnO2 nanoparticles (ii) Study of parameters affecting the adsorption process (iii) Analysis of Kinetics and Isotherms affecting the adsorption.

II. EXPERIMENTAL SECTION

2.1 Materials

The adsorption study involves the use of mentioned chemicals- MG, sulphuric acid (H_2SO_4), potassium permanganate ($KMnO_4$) purchased from Nice Pvt Ltd India and fresh sugarcane juice.

2.2 Synthesis of α-MnO_2

A simple reaction between $KMnO_4$ and sugarcane juice upon stirring and further centrifuging yields a dark brown coloured solution. This was filtered, dried and further calcinated to obtain nanoparticles of α-MnO_2.

2.3 Batch adsorption for pollutant removal

At optimum pH, dosage, concentration and the influence of time was determined for the adsorption process to happen. After filtration the amount of dye removed was found using the formula below

$$\% \text{ Removal} = (C_i\text{-}C_f)* 100/C_i \quad (1)$$

from the results of initial and final concentration of pollutant of C_i and C_f found using UV-Visible spectrophotometer[7].

III. EFFECTS AND RESULTS

3.1 Effect of pH

The pH of pollutant was varied from 2 to 6 and it was assured that λ= 611 nm for MG in the given pH range through UV-visible spectrum. The optimum pH for MG was taken 6 though better results were obtained at pH 2.4. The optimum removal at acidic pH and identical trends for removal of MG have been obtained in previous researches[8–10]. The better removal at acidic pH could be due hydrogen ions which cover the surface of adsorbent and enhances the chances of formation of bonds with the pollutant. Figure 1 gives a better idea about the changes in removal of MG with varying pH.

Revised Manuscript Received on November 08, 2019.

***** Correspondence Author

Annu T Mathew, School of Civil Engineering, Vellore Institute of Technology, Vellore, Tamilnadu, India

Saravanakumar MP, Department of Environment and water resource, School of Civil Engineering, Vellore Institute of Technology, Vellore, Tamilnadu, India

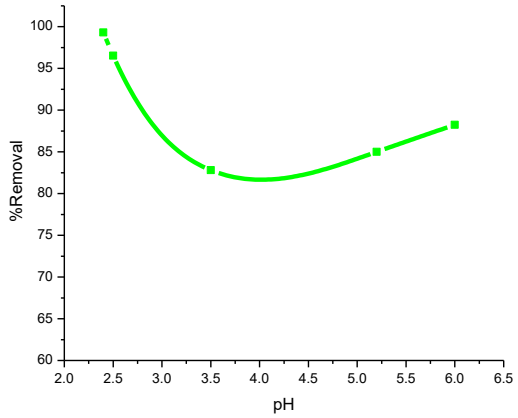

Figure 1. pH vs Percentage Removal

3.2 Effect of Dosage

For MG removal the dosage range was differed from 0.0075 g/100 mL to 0.105 g/100 mL which yields an increasing efficiency (upto 88.75%) until it reaches equilibrium at a dosage of 0.105 g/100 mL. This was plotted in the Figure 2 for adsorption of MG. The increasing trend in efficiency could be an indication of active sites being occupied by the pollutants until it reaches saturation. At the saturation point, with increase in dosage no further improvement in removal happens as the surface area and pores have already been occupied by the pollutants.

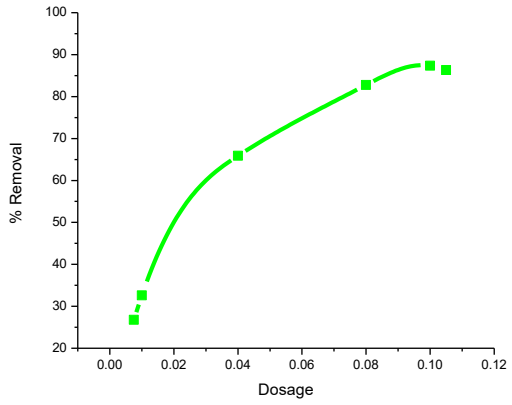

Figure 2. Dosage vs Percentage Removal

3.3 Effect of Pollutant Concentration

MG concentrations were spanned from 50mg/L to 300mg/L providing varying removal at optimum pH and dosage. The optimum concentration of MG was obtained 100 mg/L as efficiency of 99.6% was achieved at pH 2.4. The nature of curve obtained with variation of concentration at pH = 2.4 for MG is shown in Figure 3. From the nature of curve it is observed that an increase in removal was found until it reaches the optimum value and then it decreased. The initial increase of efficiency till the optimum concentration is due to greater concentration gradient. Below the optimum concentration the wide surface area of adsorbent is available for the numerous pollutant particles which provides lesser efficiency.

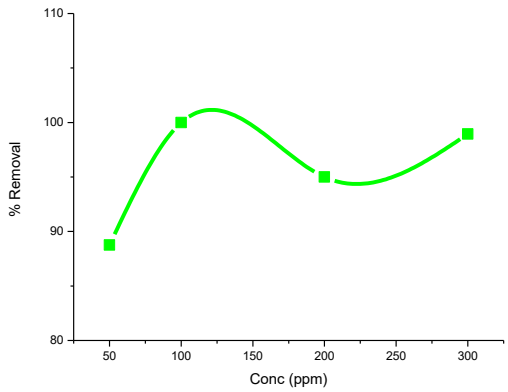

Figure 3. Concentration vs % Removal

3.4 Effect of Contact Time

For MG at pH 2.4, the optimum time was 0.5 hours providing 99.6% removal while at 2.5 hours removal was 98.66%. At pH 6 the optimum removal percentage was found at 2.5 hours with an increasing trend till saturation. Figure 4 explains the nature of the plot where due to lower internal diffusion resistance the pollutant stick to the surface of α-MnO_2 on a rapid pace but eventually on attaining saturation the active sites are totally occupied leading to decrease in efficiency.

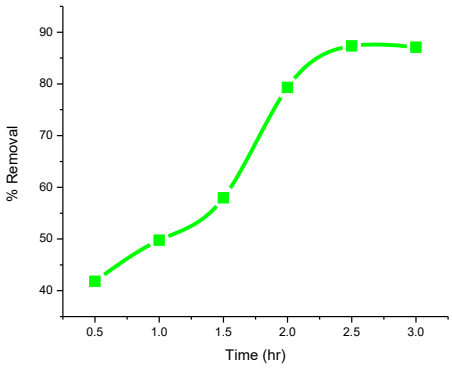

Figure 4. Time vs %Removal

3.5 Adsorption Isotherms

The Langmuir isotherm of type 2 represents a linearized plot of $1/q_e$ and $1/C_e$ (R^2= 0.9894) yielding utmost adsorption capacity as 303.03 mg/g (Table 1). Since the R_L values lies in the span of 0 and 1 it is a favorable adsorption. The K_L values presented in the table denote the affinity of pollutants to the adsorbate. The Freundlich isotherm indicate surface physisorption as it does not provide any information about saturation of the adsorbent surface. This indicates heterogeneity and exponential distribution of active sites and energy [11]. A straight plot (R^2= 0.9613) between $\log q_e$ and $\log C_e$ provides slope as 1/n (0.4851) which shows a normal adsorption as 1/n is positioned between 0 and 1. The value of $\log K_f$ intercept shows adsorption capacity (K_f) as 27.34 mg/g. The linear (R^2= 0.9608) Temkin plot between q_e and $\ln C_e$ shows the slope B (70.342 $J.mol^{-1}$) associated to the heat of adsorption and A_T (0.299 J/mol) which provides information about maximum binding energy

for pollutant. The Langmuir isotherm achieves the highest R^2 which explains the best mechanism that would have contributed to the monolayer adsorption on the nanorods. Similar trends were observed by other previous researches[12].

Table 1: Adsorption Isotherm

Pollutant	Langmiur				Freundlich			Temkin		
	Q_0(mg/g)	K_L(L/mg)	R_L	R^2	K_f(mg/g)	n	R^2	A_T(L/g)	B(J/mol)	R^2
MG	303.03	0.0345	0.19	0.9894	27.34	2.06	0.9613	0.299	70.342	0.9608

3.6 Adsorption Kinetics

A plot between $\ln(q_e-q_t)$ versus t yielded Lagergren rate constant k_1 as 0.035 min^{-1} for adsorption of MG. The $(q_e)_{cal}$ (110.713 mg/g) and R^2 (0.97) have also been obtained. The pseudo second order constants of q_e and K_L are indicated in the Table 2 which shows the best linearized fit explaining the adsorption that occurred as the R^2 obtained was 0.9902. The graph between q_t and $t^{1/2}$ drawn using data received from experiment were fit for intraparticle diffusion model. A two-step intraparticle diffusion occurs during the adsorption of pollutant on alpha MnO_2. The resistance of boundary layer could be observed as the line used to fit the model in initial step could not pass through origin. The variation of mass transfer with passage of time was seen in the first and second step with the deviation of fit line. The initial step depicts macro-pore diffusion and the second step indicates the micro-pore diffusion. The adsorption was influenced by pore diffusion, bulk diffusion and intraparticle diffusion as per the model. The slope 'k' observed in first phase was higher than second phase and the intercept 'c' in phase 1 was lower than phase 2 as has been tabulated (Table 2). Also R_1^2 value for phase 1 had a greater linearity than R_2^2 for phase 2. The rate constants α and β for Elovich model were found by a plot between q_t and lnt. It was found that α (5.274 mg/g/min) and β (0.0394 g/mg) had a regression value (0.96). Similar kinetic trends were obtained by other researches[2][13]. The correlation coefficient R^2 evaluates the suitability of the data available from the experiments and the q_e value obtained is closer to that obtained experimentally. Hence it is clear that pseudo second order fits best for removal of MG through αMnO_2.

Table 2: Adsorption Kinetics

Pollutant	Concentration	$(q_e)_{exp}$	Pseudo-first order			Pseudo-second order			Elovich			Intra-particle Diffusion		
			(q_e)cal	K_1	R^2	(q_e)cal	K_2	R^2	α	β	R^2	k_{ia},k_{ib}	c_a,c_b	R_a^2,R_b^2
	(mg/L)	(mg/g)	(mg/g)	(1/ min)		(mg/g)	(g/ ng/min)		(mg/g /min)	(g/mg)		(mg/g/ min)	(mg/g)	
MG	100	84.523	110.71	0.035	0.97	109.89	$2.2x\ 10^{-4}$	0.9902	5.274	0.0394	0.96	6.99, 1.90	8.77, 61.27	0.9769, 0.9047

IV. CONCLUSION

1. This study concludes the removal of MG by αMnO2 adsorbent. An efficient and low cost adsorbent was created using sugarcane juice which is easily available in nature.
2. The variation of pH of solution, dosage of αMnO2, concentration of dye and time affected the process of adsorption.
3. The adsorption isotherms were analyzed to conclude that Langmuir isotherm shows the best fit.
4. Various Kinetic models were examined to conclude that pseudo second order model explains the best possible adsorption kinetics that might have occurred.

REFERENCES

1. M. Baek, C. O. Ijagbemi and D. Kim, "Removal of Malachite Green from aqueous solution using degreased coffee bean," Journal of Hazardous Materials, vol. 176, pp. 820–828, 2010.
2. B. H. Hameed and M. I. El-khaiary, "Malachite green adsorption by rattan sawdust : Isotherm , kinetic and mechanism modeling," Journal of Hazardous Materials, vol. 159, pp. 574–579, 2008.
3. S. Srivastava, R. Sinha, and D. Roy, "Toxicological effects of malachite green," Aquatic Toxicology, vol. 66, pp. 319–329, 2004.
4. W. Xu, Y. Song, K. Dai, S. Sun, G. Liu, and J. Yao, "Novel ternary nanohybrids of tetraethylenepentamine and graphene oxide decorated with MnFe 2 O 4 magnetic nanoparticles for the adsorption of Pb (II)," Journal of Hazardous Materials, vol. 358, no. June, pp. 337–345, 2018.
5. Y. Huang, C. Han, Y. Liu, M. Nadagouda, L. Machala, K. E. O' Shea, V. K. Sharma and D. D. Dionysiou "Degradation of atrazine by ZnxCu1−xFe2O4nanomaterial-catalyzed sulfite under UV–vis light irradiation: Green strategy to generate SO4[rad]−," Applied Catalysis B: Environmental., vol. 221, pp. 380–392, 2018.
6. H. A. Salam, P. Rajiv, M. Kamaraj, P. Jagadeeswaran, S. Gunalan, and R. Sivaraj, "Plants : Green Route for Nanoparticle Synthesis," International Research Journal of Biological Sciences, vol. 1, no. 5, pp. 85–90, 2012.
7. E. M. Fakhry, "Padina pavonica for the Removal of Dye from Polluted Water," American Journal of Plant Sciences, vol. 2013, no. October, pp. 1983–1989, 2013.
8. S. Hashemian, A. Dehghanpor, and M. Moghahed, "Synthesis and Characterization of Manganese Ferrite Spinel for Adsorption of Malachite Green from Water," Oriental Journal of Chemistry, vol. 31 no. (3), pp. 1767-1772, 2015.
9. X. Zhang, S. Zhang, B. Pan, M. Hua, and X. Zhao, "Bioresource Technology Simple fabrication of polymer-based Trametes versicolor laccase for decolorization of malachite green," Bioresource Technology, vol. 115, pp. 16–20, 2012.
10. B. Cuiping, X. Wensheg, F. Dexin, X. Mo, G. Dong, G. Zhongxue and Z. Yanshui "Efficient decolorization of Malachite Green in the Fenton reaction catalyzed by [Fe (III) -salen] Cl complex," Chemical Engineering Journal., vol. 215–216, pp. 227–234, 2013.
11. A. C. Arampatzidou and E. A. Deliyanni, "Journal of Colloid and Interface Science Comparison of activation media and pyrolysis temperature for activated carbons development by pyrolysis of potato peels for effective adsorption of endocrine disruptor bisphenol-A," Journal of Colloid Interface Science, vol. 466, pp. 101–112, 2016.

12. B. H. Hameed and M. I. El-khaiary, "Kinetics and equilibrium studies of malachite green adsorption on rice straw-derived char," Journal of Hazardous Materials, vol. 153, pp. 701–708, 2008.
13. B. H. Hameed and M. I. El-khaiary, "Batch removal of malachite green from aqueous solutions by adsorption on oil palm trunk fibre : Equilibrium isotherms and kinetic studies," Journal of Hazardous Materials, vol. 154, pp. 237–244, 2008.